Short communication

Elastic modulus and hydraulic permeability of MDCK monolayers

K.D. Schulze [a], S.M. Zehnder [a], J.M. Urueña [a], T. Bhattacharjee [a], W.G. Sawyer [a,b],
T.E. Angelini [a,c,d,*]

[a] Department of Mechanical and Aerospace Engineering, University of Florida, Gainesville, FL, United States
[b] Department of Material Science and Engineering, University of Florida, Gainesville, FL, United States
[c] J. Crayton Pruitt Family Department of Biomedical Engineering, University of Florida, Gainesville, FL, United States
[d] Institute for Cell Engineering and Regenerative Medicine, University of Florida, Gainesville, FL, United States

ARTICLE INFO

ABSTRACT

The critical role of cell mechanics in tissue health has led to the development of many *in vitro* methods that measure the elasticity of the cytoskeleton and whole cells, yet the connection between these local cell properties and bulk measurements of tissue mechanics remains unclear. To help bridge this gap, we have developed a monolayer indentation technique for measuring multi-cellular mechanics *in vitro*. Here, we measure the elasticity of cell monolayers and uncover the role of fluid permeability in these multi-cellular systems, finding that the resistance of fluid transport through cells controls their force–response at long times.

1. Introduction

The material properties of the cytoskeleton and the cell as a whole correlate with cell behavior and tissue-level physiology (Discher et al., 2005). Numerous experimental methods for measuring the material properties of cells at local spatial scales exist. Measurements at sub-cellular length-scales have been performed by attaching super-paramagnetic beads to the cytoskeleton and applying a torque with a magnetic field (Bursac et al., 2005; Wang et al., 2002). Indentations have been performed on the actin cortex using atomic-force microscopes, also at the sub-cellular length-scale (Mahaffy et al., 2000; Sen et al., 2005). Whole cells have been stretched between micro-cantilevers (Fernández et al., 2006) and within optical traps (Guck et al., 2005). Some of these single-cell methods have been applied to cells in monolayers to gain insight into tissue-level multi-cellular mechanics (Trepat et al., 2006). Within tissues, cell groups are often under compression, and may exhibit collective mechanical responses different from those previously determined from local shear and tensile testing methods. Thus, *in vitro* measurements of cells under compression at the multicellular scale may reveal unexplored forces potentially at play within tissues.

Here we apply gentle, direct contact forces to Madin Darby Canine Kidney (MDCK) cell monolayers, compressing cell groups with steady forces and with no apparent cell damage. At short times, we determine an elastic modulus of 33.0 kPa, which drops to 15.6 kPa when the cytoskeleton is relaxed with blebbistatin. Over long times, the cells under the indenter compress slowly without translating, indicating that fluid driven out from under the contact at a rate limited by the monolayer's permeability. We combine Darcy's law with a contact mechanics model for thin layers to determine the monolayer permeability. These results show that while cell elasticity may dominate force–response in tissues at short times, dissipative resistance to fluid flow controls tissue response at long time-scales.

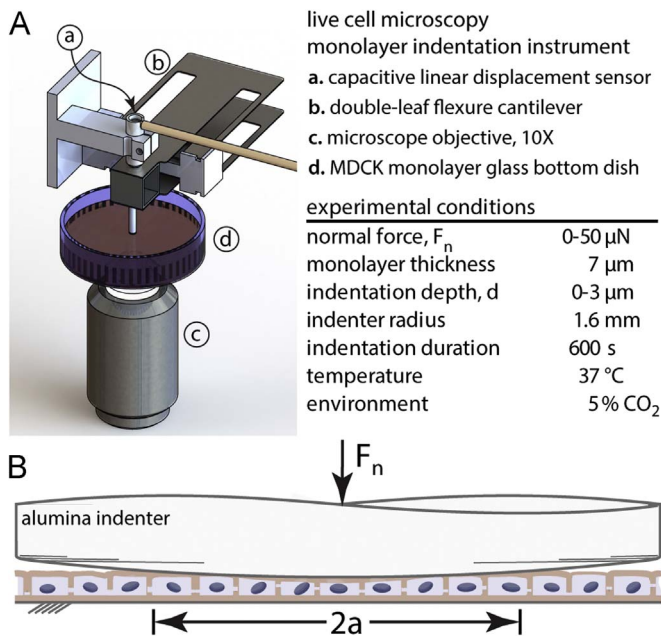## 2. Methods and materials

2.1. Cell culture protocols

MDCK cells are cultured in Dublecco's modified Eagle's media supplemented with 10% fetal bovine serum and 1% penicillin streptomycin at 37 °C in a 5% CO_2 atmosphere. Monolayer islands, 3–5 mm in diameter, are spotted onto fibronectin coated, glass-bottomed culture dishes and fluorescently dyed with 5-chloromethyl-fluorescein diacetate (CMFDA). Detailed protocols for creating monolayer islands, fluorescent labelling, and several different pharmaceutical treatments employed in this study can be found in the Supplementary information.

2.2. In situ monolayer indentation

To perform tests on monolayers, we designed a micro-indentation system delicate enough to deform cells without damage, using a maximum force of 50 µN (Fig. 1). At this load, the contact width is about 250 µm, so the average pressure

* Corresponding author at: Department of Mechanical and Aerospace Engineering, University of Florida, 338 MAE-B, Gainesville, FL 32611, United States. Fax: +1 352 392 6565.
  E-mail address: t.e.angelini@ufl.edu (T.E. Angelini).

A

live cell microscopy
monolayer indentation instrument
a. capacitive linear displacement sensor
b. double-leaf flexure cantilever
c. microscope objective, 10X
d. MDCK monolayer glass bottom dish

experimental conditions

normal force, F_n	0-50 μN
monolayer thickness	7 μm
indentation depth, d	0-3 μm
indenter radius	1.6 mm
indentation duration	600 s
temperature	37 °C
environment	5 % CO_2

B

Fig. 1. (A) A micro-indenter is positioned over an inverted microscope and translated vertically with a piezo driven stage. Deflection of the double-leaf flexure is measured with a capacitive linear displacement sensor (3 nm resolution). A constant load is held with closed-loop feedback. (B) The 1.6 mm radius indenter presses into the 7 μm thick cell layer, applying a normal force, F_n, making a contact diameter 2a. The true disparity between the indenter radius and the monolayer thickness is much greater than illustrated here.

under contact is about 1 kPa, or roughly 1/10 the typical modulus of epithelial tissue (Fig. 2). We are able to repeatedly apply direct pressure to monolayers, hold a normal load, and retract without observing any cell damage (Fig. 2B–D). To eliminate adhesion to the cells, the indenter tip is coated in f-127 pluronic before each experiment. Each of the tests described below were performed on three different monolayers.

2.3. Indentation sequence for monolayer studies

To measure the monolayer response to contact forces, we rapidly ramp the applied load from 0 to 50 μN over a 10 s period, hold for 600–700 s, and remove the load by retracting the indenter. We see the indentation depth rise rapidly without any apparent lag as the force is ramped to 50 μN, then continue to rise slowly as the force is held – a behavior reminiscent of poroelastic materials under applied step-loads. Previously, we observed water passing between MDCK cells under low pressures over long times (Zehnder et al., 2015a, 2015c), further leading us to treat the monolayers as poroelastic in the analysis described here. To characterize poroelastic materials, experiments are typically split into three different regimes of mechanical response: short times, where no fluid can flow and the material is incompressible, having a Poisson's ratio of $\nu = ½$; long times where flow has stopped and equilibrium levels of compression are achieved; intermediate times where permeability limits the rate of indentation (Hu et al., 2010). At short times, since ν is known, $E^* = E/(1 - \nu^2) = 4/3E$, where E^* is the contact modulus and E is Young's modulus. This modulus is typically used again for analysis at long times to determine ν at equilibrium after flow has stopped. Here we follow the same protocol, but we

do not attempt to determine ν because the internal cell architecture may evolve over very long times. Indentation tests with simultaneous imaging of the cytoskeleton are required to study the long time limit of a poroelastic interpretation of mechanical data.
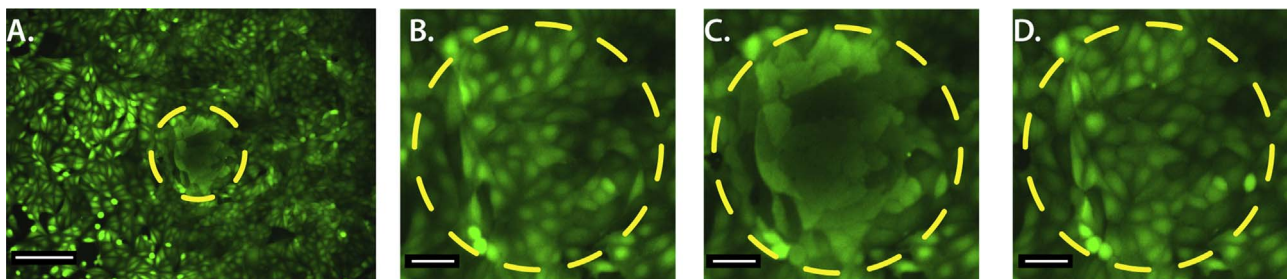
3. Results

3.1. Thin slab contact mechanics of monolayers

At the start of the indentation protocol, the contact width, a, grows rapidly with indentation depth, d, due to the large disparity between the indenter radius (1.6 mm) and the monolayer thickness (7 μm). For example, a exceeds the layer thickness when d is just 15 nm. Thus, the 3D elasticity problem studied here falls within a thin slab limit that can be described by the Winkler elastic foundation model (Johnson, 1985). In this limit, for a spherical indenter pressing on a thin sheet of thickness h and contact modulus E^*, the relationship between normal force, F_n and indentation depth is given by $F_n = \pi E^* R h^{-1} d^2$. This relationship arises from the lateral confinement of local stresses by the rigid substrate; stresses are approximately uniform along the indentation direction and propagate laterally by the slab thickness, h. Consequently, this model will not apply to tests performed on soft substrates having an elastic modulus comparable to the cell layer.

To test whether this simple elastic slab model describes monolayer mechanics at short times, we examine the scaling between the F and d data-points during the first 10 s of indentation. We find that d^2 is proportional to F, and that data from different experiments can be collapsed onto a universal scaling curve when normalized by the constant system parameters (Fig. 3). For each measurement, E^* is determined by fitting the Winkler model to the data, with all other parameters fixed to their known quantities. Averaging across measurements performed on different monolayers, we find $E^* = 33.0 \pm 3.0$ kPa (mean $\pm$ standard deviation). Cell stiffness is linked to cytoskeletal pre-stress, driven by Myosin II, so to check whether the modulus measured here is driven by the same underlying mechanics, we repeat the experiments on cells drugged with 100 μM blebbistatin, a Myosin II inhibitor. We find $E^* = 15.6 \pm 5.5$ kPa for blebbistatin treated cells, about half that of untreated cells. At short times, when no fluid can flow, the effective Poisson's ratio is ½, allowing the Young's modulus, E, to be determined from E^*. We find $E = 24.8$ kPa and 11.7 kPa for untreated and blebbistatin treated monolayers, respectively.

3.2. MDCK monolayer permeability

In poroelastic materials, fluid permeability controls the response to applied pressure over intermediate time-scales. Our measurements reveal that this time-scale for cell monolayers is on the order of hundreds of seconds for pressures in the kilopascal
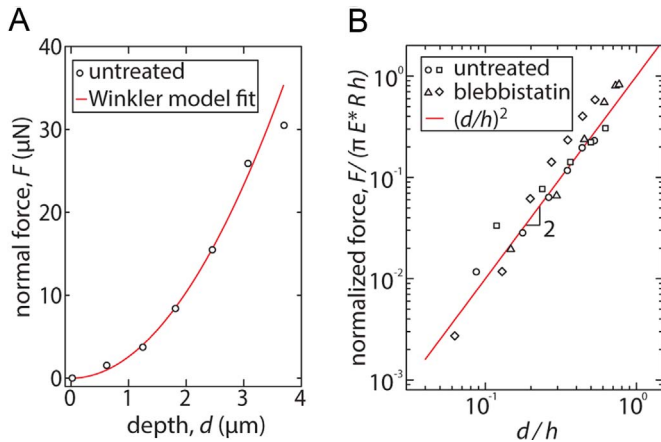

Fig. 2. (A) MDCK monolayer under persistent 50 μN load. Scale bar: 200 μm. Monolayer indentation viewed at higher magnification, before (B), during (C), and after indentation (D) is performed without apparent cell damage. Scale bar: 50 μm.

A / B

Fig. 3. (A) Representative loading curve during the first 10 s of indentation, plotting force, F, versus the indentation depth, d, for an untreated monolayer. The red line is a fit of the Winkler contact model to the data, where the contact modulus, E^*, is the fitting parameter. (B) Collapse of four different indentation data-sets of both untreated and blebbistatin treated MDCK monolayers. The datasets are collapsed by non-dimensionalizing the Winkler model F–d curve after fitting each dataset. The collapsed data scales like d^2, as predicted by the Winkler Model. (For interpretation of the references to color in this figure legend, the reader is referred to the web version of this article.)
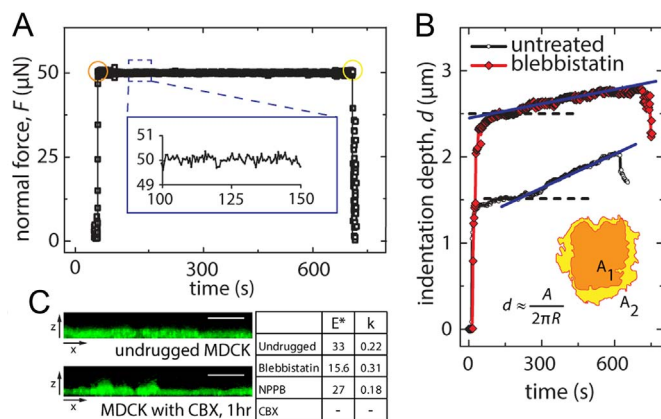

Fig. 4. (A) Force versus time curve of a typical indentation experiment at 50 μN normal load held for 600 s. (Inset) Average force fluctuations about the 50 μN persistent load are ± 1 μN for these experiments. (B) Indentation depth versus time for the indentation experiments. Following a rapid elastic deformation, the indentation depth persistently and slowly increases over the course of hundreds of seconds, consistent with poroelastic dynamics. The dashed lines demarcate the saturation point of the elastic regime and the transition into poroelastic behavior. (Inset) Representative contact area observations at the beginning of indentation (orange) and end of indentation (yellow) for the experiments, $A_1 = 37{,}000$ μm² and $A_2 = 60{,}000$ μm². Contact area increasing over time under persistent load is observed in all tested conditions. (C). (Left) Confocal microscopy X–Z scans of MDCK monolayers before and after administration of the gap junction blocker, CBX (60X magnification). The monolayer surface changes from a flat (top) to rough within one hour after CBX drugging (bottom), preventing analysis using the Winkler model. (Right) The average contact modulus and permeability of monolayers under different testing conditions. (For interpretation of the references to color in this figure legend, the reader is referred to the web version of this article.)

range. By feeding back on the capacitance probe signal, our instrument can hold a constant force of 50 ± 1 μN for these long durations (Fig. 4A). A remaining challenge, however, is the measurement of indentation depth over these time-scales during which we expect fluid to flow through the monolayer. Small variations in temperature that result in uncontrolled length changes of mechanical components make it impossible to determine micron-scale changes in indentation depth from the piezo stage position, which is moving to hold a constant force. We therefore

determine the indentation depth by analyzing images of the monolayer, measuring the area of contact between the monolayer and the hemisphere. The contact area, A, is measured with image processing code that identifies the edge of deformed regions, and we infer an average contact radius, a, from $A = \pi a^2$. For a sphere pressing into a flat surface, the contact radius can be used to determine a maximum indentation depth, d, at the center of the indent from $a = \sqrt{2Rd}$, where $R = 1.6$ mm is the radius of curvature of the hemispherical indenter.

To determine the cell layer permeability at intermediate times, we employ the surface pressure distribution from the Winkler model, given by $P(r,t) = \frac{E^*}{2Rh}(a^2(t) - r^2)$, where r is the radial distance from the center of contact. The resistance to flow of fluid out of the region directly under indentation depends on the permeability of the system, which can be defined generally by Darcy's law, which can be written in many different forms. Here, we use a form of Darcy's law that relates the local velocity, $\mathbf{v}(\mathbf{r},t)$, of fluid passing through a porous material of thickness, h, with a permeability k_{eff}, due to a local pressure gradient $\nabla P(\mathbf{r},t)$, given by $\mathbf{v}(\mathbf{r},t) = \frac{k_{eff}}{h}\nabla P(\mathbf{r},t)$. Using the Winkler pressure distribution in cylindrical coordinates, the gradient is $\nabla P(r,t) = \frac{-E^*}{Rh}r\hat{r}$. The velocity of the fluid at the edge of contact, moving outward at a flow rate Q is given by $\mathbf{v}(a,t) = \frac{Q(t)}{2\pi a(t)h}\hat{r}$, where the denominator is the surface area of a cylindrical shell below the edge of contact. Equating these velocities at the boundary, $r = a$, we solve for the permeability, finding $k_{eff} = \frac{Rh}{2E^*} \cdot \frac{Q(t)}{\pi a^2}$. We employ volume conservation to write the volumetric flow rate as $Q(t) = \pi \cdot 2Rd\dot{d}$, where $\dot{d}$ is the time derivative of the indentation depth. We use this relationship to eliminate Q in the permeability formula, finding $k_{eff} = \frac{Rh}{2E^*} \cdot \dot{d}$. A linear fit of the data (Fig. 4C) is used to determine $\dot{d}$, yielding $k_{eff} = 0.22 \pm 0.01$ μm³ kPa⁻¹ s⁻¹ for undrugged cells, and $k_{eff} = 0.31 \pm 0.03$ μm³ kPa⁻¹ s⁻¹ for blebbistatin treated cells.

In the MDCK monolayers studied here, cells are connected to one another through fluid-permeable gap junctions, which allow water, ions, and small molecules to pass between cells and are likely the limiting factor for inter-cellular fluid flow (Zehnder et al., 2015a, 2015b, 2015c). The potential mechanical coupling between cell contractility, cell morphology, and gap-junction stability may explain this modest increase in the permeability of monolayers with inhibited cytoskeletal contraction, though further investigation is required to verify such an underlying mechanism. It is also intriguing that, while the blebbistatin-treated monolayer is slightly more permeable, the indentation rate is decreased (Fig. 4B). We interpret this observation by considering that $\dot{d}$ is linearly proportional to E^*, arising from the proportionality between ∇P and E^* in the Winkler model. Thus, a lower modulus may serve as a mechanism to reduce persistent fluid flow in monolayers with increased permeability. We perform control studies to test the potential role of inter-cellular gap junction permeability. We block gap junctions by treating monolayers with Carbenoxolone (CBX), finding that large-amplitude undulations emerge at the monolayer apical surface (Fig. 4C). This surface roughness prohibits the interpretation of indentation experiments with the model developed here, so we perform a qualitative test on un-drugged individual cells. These cells rupture at applied loads of 50 μN or less, suggesting that gap-junction permeability may be essential to allowing volume change under applied mechanical pressure (see Supplementary information for experimental details). Finally, we perform a control experiment that tests the role of water exchange with the liquid bath across the cell membrane. Indentation tests on cells treated with the chloride channel blocker 5-nitro-2-(3-phenylpropylamino)-benzoic acid (NPPB) reveal a modulus and permeability comparable to that of un-drugged cells (see Supplementary information and Fig. 4C).

4. Discussion

The instrument and experimental approach developed here represent a bridge between traditional mechanical techniques, in which macroscopic slabs of tissue are stretched, sheared, or indented, and more recently developed techniques that probe individual cells, one at a time. Similar to the way that traction force microscopy was extended to the meso-scale to study multi-cellular forces (Tambe et al., 2011; Trepat et al., 2009), our meso-scale indentation method allows *in vitro* systems like monolayers to be probed as multi-cellular model tissues with the level of control needed to elucidate the basic principles of collective cell mechanics. In future work, as instrument sensitivity and *in situ* imaging improves, more advanced questions about cell monolayer contact mechanics may be explored (Ateshian, 2009; Dapp et al., 2014; Nalam et al., 2015).

In recent work, the elastic moduli of single 3T3 fibroblasts and of small islands of keratinocytes have been inferred by combining traction-force microscopy with continuum theoretical models (Mertz et al., 2012; Oakes et al., 2014), finding moduli about an order of magnitude lower than measured here. This discrepancy may reflect variation in mechanics between cell types, but may also arise from the need to perform traction force measurements on soft substrates, which softens the cells. Direct measurements of single MDCK cells with microrheological techniques also reveal a lower modulus than measured here (Balland et al., 2006), while the elastic modulus of MDCK monolayers on collagen scaffolds agree with our results (Harris et al., 2012). Thus, it will be interesting in the future to investigate how cells may stiffen upon culturing in monolayer. Here we have found a potential contributor to this difference between monolayer and single cell mechanics; the notion that fluid transport contributes to multicellular mechanics has been inferred from passive observation, but measurements of the associated forces have not been performed previously (Zehnder et al., 2015c). The permeability measured here differs by less than an order of magnitude from this previous prediction, and further indicates that the forces associated with intercellular fluid flow play a significant role in multicellular mechanics within tissues, in addition to the well-established elastic forces of the cytoskeleton.

Conflict of interest

The authors report no conflict of interest.

Sources of funding

Appendix A. Supplementary material

Supplementary data associated with this article can be found in the online version at http://dx.doi.org/10.1016/j.jbiomech.2017.01.016.

References

Ateshian, G.A., 2009. The role of interstitial fluid pressurization in articular cartilage lubrication. J. Biomech. . http://dx.doi.org/10.1016/j.jbiomech.2009.04.040

Balland, M., Desprat, N., Icard, D., Fereol, S., Asnacios, A., Browaeys, J., Henon, S., Gallet, F., 2006. Power laws in microrheology experiments on living cells: comparative analysis and modeling. Phys. Rev. E 74, 21911. http://dx.doi.org/10.1103/PhysRevE.74.021911.

Bursac, P., Fabry, B., Lenormand, G., Oliver, M., Weitz, D.A., Viasnoff, V., Butler, J.P., Fredberg, J.J., 2005. Cytoskeletal remodelling and slow dynamics in the living cell. Nat. Mater. 4, 557–561. http://dx.doi.org/10.1038/nmat1404.

Dapp, W.B., Prodanov, N., Müser, M.H., 2014. Systematic analysis of Persson's contact mechanics theory of randomly rough elastic surfaces. J. Phys.: Condens. Matter 26, 355002. http://dx.doi.org/10.1088/0953-8984/26/35/355002.

Discher, D.E., Janmey, P., Wang, Y.-L., 2005. Tissue cells feel and respond to the stiffness of their substrate. Science 310, 1139–1143. http://dx.doi.org/10.1126/science.1116995.

Fernández, P., Pullarkat, P.A., Ott, A., 2006. A master relation defines the nonlinear viscoelasticity of single fibroblasts. Biophys. J. 90, 3796–3805. http://dx.doi.org/10.1529/biophysj.105.072215.

Guck, J., Schinkinger, S., Lincoln, B., Wottawah, F., Ebert, S., Romeyke, M., Lenz, D., Erickson, H.M., Ananthakrishnan, R., Mitchell, D., Kas, J., Ulvick, S., Bilby, C., 2005. Optical deformability as an inherent cell marker for testing malignant transformation and metastatic competence. Biophys. J. 88, 3689–3698. http://dx.doi.org/10.1529/biophysj.104.045476.

Harris, A.R., Peter, L., Bellis, J., Baum, B., Kabla, A.J., Charras, G.T., 2012. Characterizing the mechanics of cultured cell monolayers. Proc. Natl. Acad. Sci. USA 109, 16449–16454. http://dx.doi.org/10.1073/pnas.1213301109.

Hu, Y., Zhao, X., Vlassak, J.J., Suo, Z., 2010. Using indentation to characterize the poroelasticity of gels. Appl. Phys. Lett. 96, 1–4. http://dx.doi.org/10.1063/1.3370354.

Johnson, K.L., 1985. Contact Mechanics. Cambridge University Press, Cambridge, pp. 104–106.

Mahaffy, R.E., Shih, C.K., MacKintosh, F.C., Kas, J., 2000. Scanning probe-based frequency-dependent microrheology of polymer gels and biological cells. Phys. Rev. Lett. 85, 880–883.

Mertz, A.F., Banerjee, S., Che, Y., German, G.K., Xu, Y., Hyland, C., Marchetti, M.C., Horsley, V., Dufresne, E.R., 2012. Scaling of traction forces with the size of cohesive cell colonies. Phys. Rev. Lett., 108. http://dx.doi.org/10.1103/PhysRevLett.108.198101.

Nalam, P.C., Gosvami, N.N., Caporizzo, M.A., Composto, R.J., Carpick, R.W., 2015. Nano-rheology of hydrogels using direct drive force modulation atomic force microscopy. Soft Matter 11, 1–3. http://dx.doi.org/10.1039/C5SM01143D.

Oakes, P.W., Banerjee, S., Marchetti, M.C., Gardel, M.L., 2014. Geometry regulates traction stresses in adherent cells. Biophys. J. 107, 825–833. http://dx.doi.org/10.1016/j.bpj.2014.06.045.

Sen, S., Subramanian, S., Discher, D.E., 2005. Indentation and adhesive probing of a cell membrane with AFM: theoretical model and experiments. Biophys. J. 89, 3203–3213. http://dx.doi.org/10.1529/biophysj.105.063826.

Tambe, D.T., Hardin, C.C., Angelini, T.E., Rajendran, K., Park, C.Y., Serra-Picamal, X., Zhou, E.H., Zaman, M.H., Butler, J.P., Weitz, D.A., Fredberg, J.J., Trepat, X., 2011. Collective cell guidance by cooperative intercellular forces. Nat. Mater. 10, 469–475. http://dx.doi.org/10.1038/nmat3025.

Trepat, X., Puig, F., Gavara, N., Fredberg, J.J., Farre, R., Navajas, D., 2006. Effect of stretch on structural integrity and micromechanics of human alveolar epithelial cell monolayers exposed to thrombin. Am. J. Physiol.: Lung Cell. Mol. Physiol. 290, L1104–L1110. http://dx.doi.org/10.1152/ajplung.00436.2005.

Trepat, X., Wasserman, M.R., Angelini, T.E., Millet, E., Weitz, D.A., Butler, J.P., Fredberg, J.J., 2009. Physical forces during collective cell migration. Nat. Phys. 5, 426–430. http://dx.doi.org/10.1038/nphys1269.

Wang, N., Tolić-Nørrelykke, I.M., Chen, J., Mijailovich, S.M., Butler, J.P., Fredberg, J.J., Stamenović, D., 2002. Cell prestress. I. Stiffness and prestress are closely associated in adherent contractile cells. Am. J. Physiol.: Cell Physiol. 282, C606–C616. http://dx.doi.org/10.1152/ajpcell.00269.2001.

Zehnder, S.M., Suaris, M., Bellaire, M.M., Angelini, T.E., 2015a. Cell volume fluctuations in MDCK monolayers. Biophys. J. 108, 247–250. http://dx.doi.org/10.1016/j.bpj.2014.11.1856.

Zehnder, S.M., Wiatt, M.K., Uruena, J.M., Dunn, A.C., Sawyer, W.G., Angelini, T.E., 2015b. Multicellular density fluctuations in epithelial monolayers. Phys. Rev. E – Stat. Nonlinear Soft Matter Phys., 92. http://dx.doi.org/10.1103/PhysRevE.92.032729.

Zehnder, S.M., Zegers, F.M., Angelini, T.E., 2015c. A Langevin model of physical forces in cell volume fluctuations. J. Biomech. . http://dx.doi.org/10.1016/j.jbiomech.2015.12.051